HOKKAIDO UNIVERSITY

Title	Temperature Inversions off the Eastern Coast of the Oshima Peninsula, Hokkaido.
Author(s)	MIYAKE, Hideo
Citation	北海道大學水産學部研究彙報, 33(3), 135-148
Issue Date	1982-09
Doc URL	https://hdl.handle.net/2115/23794
Type	departmental bulletin paper
File Information	33(3)_P135-148.pdf

Hokkaido University Collection of Scholarly and Academic Papers : HUSCAP

Bull. Fac. Fish. Hokkaido Univ.
33(3), 135–148. 1982.

Temperature Inversions off the Eastern Coast of the Oshima Peninsula, Hokkaido.*

Hideo MIYAKE**

Abstract

Temperature inversions generating off the eastern coast of the Oshima peninsula, Hokkaido, were observed from June to September, and the characteristics, physical quantities and density stratification of the layers are discussed. Throughout June, thick inversion layers with mean thickness of about 24 m were observed from the middle layer of the sea to near the sea bottom. The layers in July were characterized by less thickness ($\approx$14 m) with high gradients in both temperature and salinity (0.08°C m^{-1}, 0.03 ‰ m^{-1}). Differences in characteristics between June and July were explained by the inflowing pattern of two different oceanic waters. From the stability analysis, inversion layers in June were sufficiently compensated for by the salinity increase, and this might provide one of the reasons that inversion layers are of long duration in spring.

Introduction

Oceanic conditions in Funka Bay and off the eastern coast of the Oshima peninsula, Hokkaido, are characterized by the replacement of two major water masses once a year; the Oyashio Water and the Tsugaru Warm Water[1–5]. Since the properties of these oceanic waters are different in both temperature and salinity, many types of thermohaline structures (*e.g.*, a coastal front[5], a temperature inversion [5–7] and a warm salty intrusion[6]) are formed due to the inflowing oceanic waters of the coastal region. They can be easily found by field observation, since the phenomena are well localized in space and time.

It may be important to investigate such structures from the standpoint of variations in coastal hydrography and of the formation of coastal water masses, since the mixing processes between two different water masses may generate these structures. However, previous studies have shown little about their physical aspect in the region. This paper deals with temperature inversions as one of the thermohaline structures. The characteristics and physical quantities of temperature inversions in different hydrographic conditions are firstly described, and stratifications of these layers are secondly considered. The actual mechanism of their formation associated with the mixing process, such as Fedorov mentioned[8], is discussed very little.

---

* *Contribution No. 149 from the Research Institute of North Pacific Fisheries, Hokkaido University*

** *Research Institute of North Pacific Fisheries, Faculty of Fisheries, Hokkaido University.*
(北海道大学水産学部北洋水産研究施設)

Surveyed region, methods and data

Fig. 1 shows the location of stations, which are within 15 miles of the eastern coast of the Oshima peninsula. Ohtani *et al.*[1,3–5] and Ohtani[2] showed that two oceanic source waters and two kinds of bay waters which are individually formed in the bay through the transformation of source waters occupy the region from spring to autumn. As for the source waters, they are the Tsugaru Warm Water (Tw: $T>6°C$, $S>33.6‰$) and the Oyashio Water diluted with

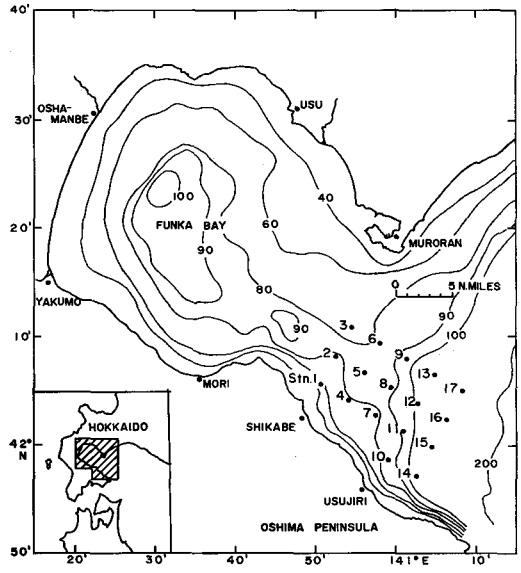

Fig. 1. Location of stations and bathymetry of surveyed region. Numbers indicate water depth in meters.

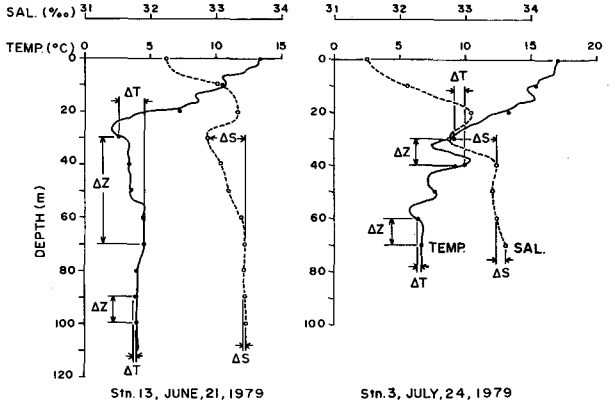

Fig. 2. Notation of the temperature inversion characteristics. Solid and open circles denote values of temperature and salinity respectively, as obtained with Nansen cast. Solid lines of vertical temperature profile are drawn by the BT traces in these cases.

melting ice (O & Oi; $T<2\sim3°C$, $32.0<S<33.3$ ‰); the bay waters are clarified as the Summer Surface Funka Bay Water (Fs; $S<32.0$ ‰) and the Winter Funka Bay Water (Fw; $3<T<6°C$, $S>33.8$ ‰). Both O & Oi and Tw flow counter-clockwise into the bay from the northeastern side near Muroran, and a remarkable front is formed between the inflowing oceanic water and the outflowing bay water along the peninsula. This makes the oceanic conditions considerably more complicated.

The observations were made from June to September in 1978 and 1979 by the RV Ushio Maru (98 GT) of the Faculty of Fisheries, Hokkaido University. Nansen hydrographic casts were made at 10 m vertical intervals, at stations situated 3 miles away from each other as shown in Fig. 1. Because of the rough weather, only 6 casts were made in August of 1979.

On the basis of the data obtained with the Nansen casts, temperature inversions with the increment of larger than 0.05°C, which exceeds the accuracy of the reversing thermometer, were used for the analysis. If the inversion layer continues vertically deeper than 10 m, we regard it as one layer as shown in Fig. 2. We denote in Fig.2 by ΔZ the thickness of the inversion layer, by ΔT the temperature difference across the layer and ΔS the corresponding salinity difference.

Characteristics of temperature inversions

1. *Hydrographic conditions*

In relation to the water mass classification mentioned above, two different hydrographic conditions are examined for June and July, with respect to temperature inversions. From Figs. 3 and 4, it was observed clearly that the water from the surface to 30 m depth in June began to change in nature from O&Oi to a transitional condition toward Fs. In particular, the surface layer along the peninsula changed to warm ($T>8\sim10°C$) and less saline ($S<32.0$‰) water. The water ($T>4°C$, $S>33.4$‰) which was found in the deep layer of Stns. 13 and 17, suggested that Tw was close to this region. However, O&Oi dominated in the water column between 40 m and about 90 m depth. Both the horizontal gradients in temperature and salinity were small below 40 m depth.

Since the coldest layer, about 2°C, extended horizontally at a depth of 50 m, the layer increased gradually in temperature as it approached the bottom. The salinity, however, tended to increase gradually with depth; hence the density stratification was stable. Similar features were observed from March to June in this region.[5)]

Figs. 5 and 6 indicate that the oceanographic condition changed rapidly in July, when Tw flowed into the surveyed region. Namely, in the surface layer, Fs existed in the bay mouth and along the peninsula, forming a front with salty ($S>33.0$ ‰) offshore water. However, in the middle layer, Tw intruded into the cool ($T<6\sim8°C$) coastal water from offshore, as a horizontal layer of warm salty water.

Under such oceanographic conditions, most temperature inversions were found in the upper half of the warm salty intrusion with the maximum salinity at the lowest layer. Since the temperature and salinity gradients increased both in

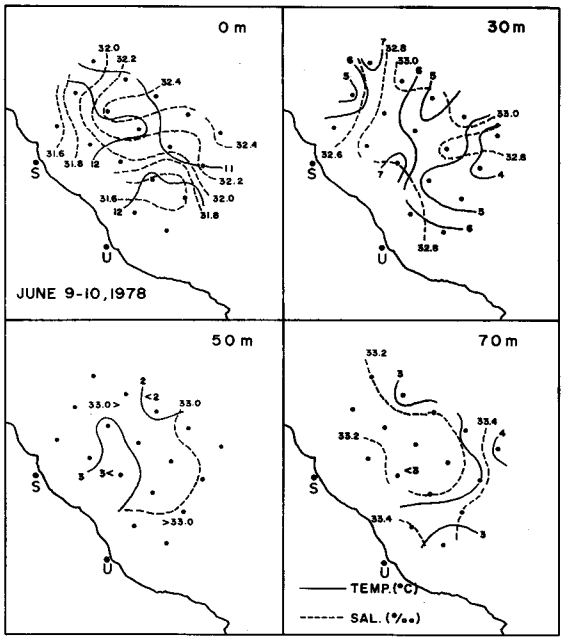

Fig. 3. Horizontal distribution of temperature and salinity on June 9 and 10, 1978, at 0, 30, 50, and 70 m depth.

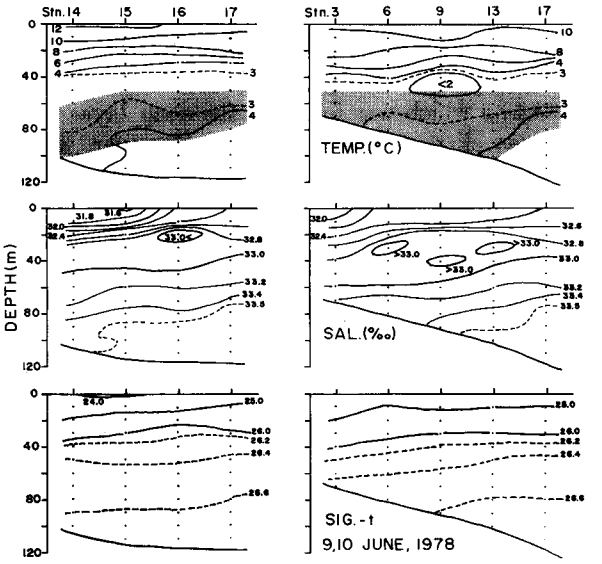

Fig. 4. Vertical sections of temperature, salinity and sigma-t in June 1978. Temperature inversion layers are shaded.

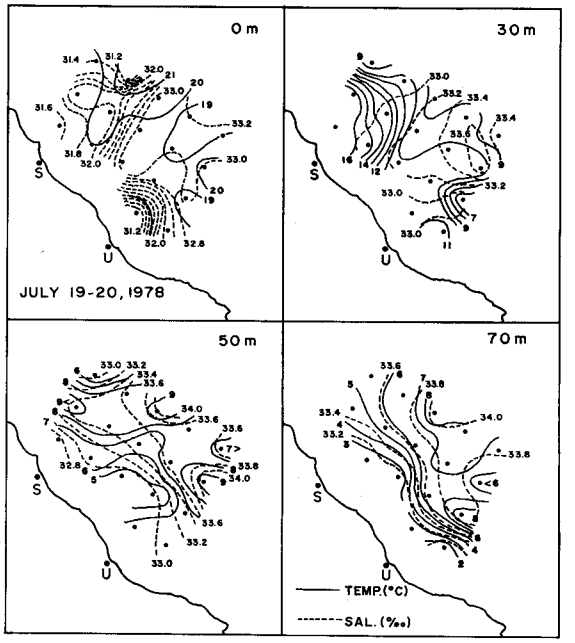

Fig. 5. Horizontal distribution of temperature and salinity on July 19 and 20, 1978, at 0, 30, 50 and 70 m depth.

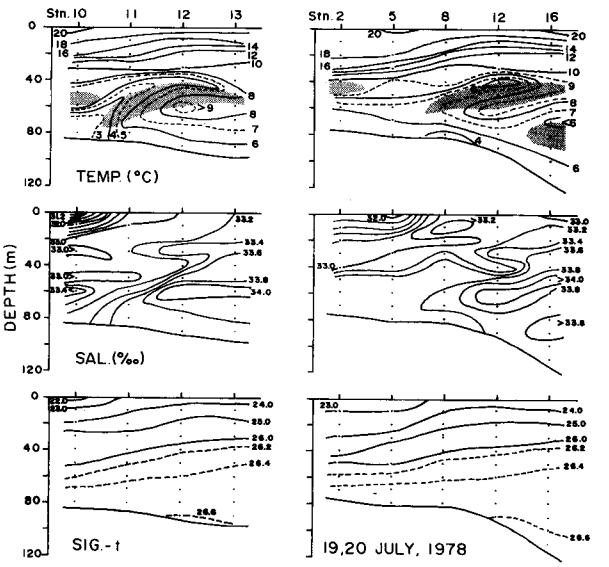

Fig. 6. Vertical sections of temperature, salinity and sigma-t in July 1978. Temperature inversion layers are shaded.

horizontal and vertical, the inclination of isopycnal lines became large. The cool ($T<3°C$) and less saline ($S<33.3‰$) water which existed below 70 m depth along the peninsula corresponded to O&Oi.

Tw occupied almost half the vertical section in the middle layer in August, and inversions similar to those in July were recognized. In September, Tw covered the whole region except the surface and bottom layers. Though the layers with the maximum salinity still remained, temperature inversions associated with the horizontal intrusion were rare. Most inversions appeared in the surface layer in this period.

2. *Inversion layers on a TS-diagram*

Fig. 7 shows the temperature inversion layers plotted on TS-diagrams, in which the ranges of water masses are also indicated with symbols. Temperature inversions generated in water of temperature higher than 13°C are omitted here, since they might be due to the cooling of the surface layer.

Most of the inversion layers in June fell within the narrow range of 2.0°C to 5.0°C in temperature and of 32.5‰ to 33.5‰ in salinity. Particularly, temperature inversions in June of 1978 were concentrated in the range between the two points of 1.5°C, 32.7‰ and 5.0°C, 33.8‰, having a width of ±0.5°C, as

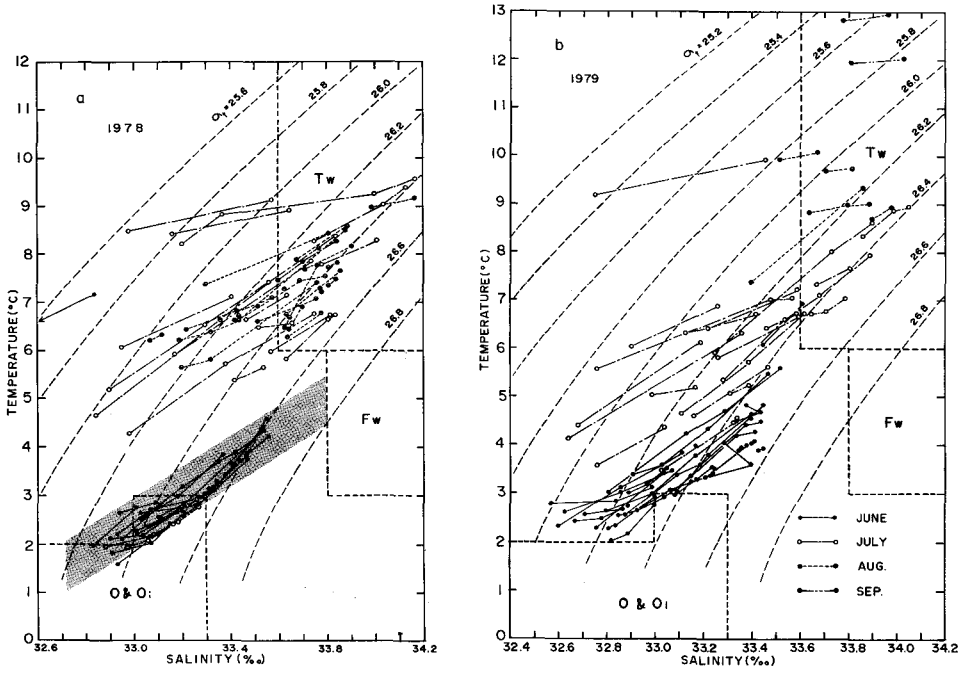

a. b.

Fig. 7. Temperature inversions on the TS-diagrams and the water mass classification. O&Oi, Tw and Fw indicate the Oyashio Water, the Tsugaru Warm Water and the Winter Funka Bay Water, respectively.

pointed out by Ohtani and Kido[5]. This area is shaded in Fig. 7-a. Inversion layers in June, which were confined to this narrow range, show the result of linear mixing between O&Oi and Fw.

From Figs. 5 and 6, it is clear that Tw intruded into the middle layer in July; however, O&Oi still remained near the sea bottom along the peninsula. This made the inversion characteristics two different types. One was the inversion layers near the bottom, which were associated with O&Oi; hence they were identified with a group which was formed by the inversion layers generated in June. The other was these in the middle layer, which were distributed over the wide range between 4.0°C and 10.0°C in temperature, and between 32.6‰ and 34.2 ‰ in salinity. Each inversion layer tended to have a large salinity difference. The deepest layers appeared to terminate in and near the water of Tw. This suggests that they generated at the same time when Tw flowed in.

Such inversion associated with Tw could be observed in August as well. However, their extent on the TS-diagram was small and most of them were found in the water of Tw.

3. *Depth and thickness of the inversion layers*

Fig. 8 shows the thickness of the inversion layers in June and in the following three months for both years, with respect to the depths of occurrence. In June, the inversion layers were distributed over several depths and had various thicknesses. Thick layers ($\Delta Z \geqq 30$ m) were found below the depth of 30 m, which accounted for 40% of the total data. Considering that the water depth in the region ranged from about 70 m to 120 m, these inversions in the middle layer might have extended to near the sea bottom.

On the other hand, in July and August inversion layers having a 10 m mode thickness were found mainly in the layer between 50 m and 70 m depth, and their number decreased exponentially with increasing thickness. The number of thin layers ($\Delta Z \leqq 20$ m) accounted for 77% of the total data, and layers of 10 m in

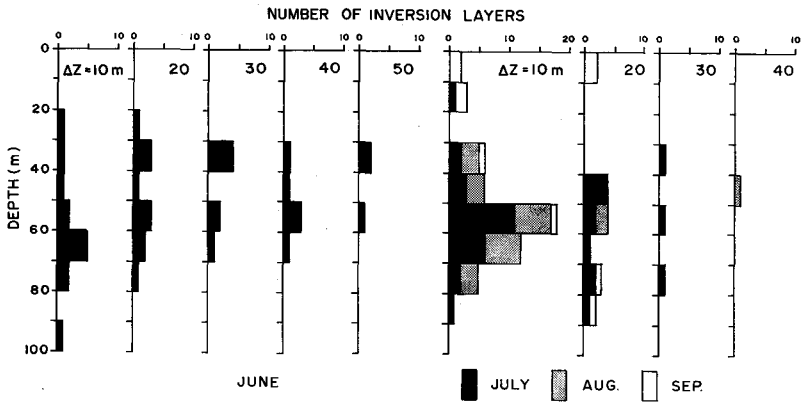

Fig. 8. Frequency distribution of the thickness of temperature inversion layers with respect to depth of occurrence.

thickness existing from 50 m to 70 m depth occupied 41% of this total. Thus, temperature inversions in the middle layer were characterized by less thickness in July and August. Referring to the hydrographic conditions described earlier, their depth of occurrence corresponded to the inflowing layer of Tw, and their thickness was about half of the intrusive layer. In September, the layers occurred mostly in the subsurface layer.

4. *Physical quantities of the temperature inversion layers*

Table 1 shows the mean physical quantities over the observational period. Temperature and salinity in the layers changed from values close to those of O&Oi in June to those of Tw in August, and in July they showed intermediate values between O&Oi and Tw. In June and July temperature and salinity differences in the layers were of the same order, about 1.1°C and 0.4‰ respectively, though the thicknesses of the layers were different. Therefore, in July, the vertical gradients in temperature and salinity, and the static stability, doubled to as large as these of June. Inversion layers in July had vertical gradients of about 0.08°C m^{-1} in temperature and of 0.03 ‰ m^{-1} in salinity.

Tmperature inversions under the condition of decreasing temperature with depth, as shown in the right-hand graph of Fig. 2, might be underestimated, since data were taken at 10 m intervals. Therefore, the differences mentioned above may actually be larger than those presented here if continuous data such as BT or CTD are used.

In August and September, the thickness of inversion layers and their differences in both temperature and salinity decreased gradually. However, the static stability increased rapidly in September, since the occurrence of inversion layers was concentrated in the covenctional layer under the surface, where the vertical gradient of salinity was the largest in water columns.

Table 1. *Physical quantities of temperature inversion lvyers for various periods.*

Date	Nos. of Layer	$\overline{T}$ °C	$\overline{S}$ ‰	$\overline{\Delta Z}$ m	$\overline{\Delta T}$ °C	$\overline{\Delta S}$ ‰	$\overline{\Delta T}/\overline{\Delta Z}$ $\times 10^{-2}$ °C m^{-1}	$\overline{\Delta S}/\overline{\Delta Z}$ $\times 10^{-2}$ ‰ m^{-1}	$\overline{E}$ $\times 10^{-8}$ c.g.s.
June									
1978, 9–10	17	3.13	33.14	24.7	1.15	0.36	4.66	1.46	8.25
1979, 21–23	23	3.59	33.12	23.0	1.16	0.36	5.04	1.57	7.85
Total	40	3.39	33.13	23.8	1.15	0.36	4.83	1.51	8.02
July									
1978, 19–20	18	6.30	33.45	14.4	1.07	0.42	7.43	2.92	14.34
1979, 23–24	21	6.69	33.31	13.8	1.03	0.40	7.46	2.90	16.00
Total	39	6.51	33.38	14.1	1.05	0.41	7.45	2.91	15.23
August									
1978, 25–26	20	7.26	33.64	12.5	0.71	0.23	5.68	1.84	7.37
1979, 16–17	5	9.16	33.74	12.0	0.53	0.21	4.42	1.75	6.66
Total	25	7.46	33.66	12.4	0.67	0.22	5.40	1.77	7.22
September									
1978, 25–26	3	15.26	33.66	13.3	0.47	0.39	3.53	2.93	29.00
1979, 25–26	6	16.38	33.61	13.3	0.19	0.21	1.43	1.58	9.23
Total	9	16.02	33.63	13.3	0.28	0.27	2.11	2.03	15.82

These differences of characteristics in the inversion layers are caused by the inflowing pattern of oceanic waters[5]. Namely, O&Oi flows in over Fw, the two having significant density differences, while Tw intrudes into the middle layers of variable density and takes the form of horizontal intrusion, since Tw and O&Oi have similar densities at each level. Consequently, thick inversion layers with moderate temperature gradients were widely formed in June. On the other hand, thin inversion layers, having both steep temperature and salinity gradients, extended like warm tongues from offshore to near the coast in July and August.

Stratification of the temperature inversion layers

1. *Static stability parameters*

Fedorov[9] explained the differences of temperature inversions between the Okhotsk Sea and the Atlantic Ocean by a method of static stability analysis. Howe and Tait[10] argued for the mixing process of the Mediterranean Water and the Atlantic Water in the same manner.

Fedorov's method is applied to the data here to consider the density stratification of inversion layers in a variety of oceanographic conditions. The relationship between ΔT and ΔS in the inversion layers is represented by the following regression rule,

$$\Delta S = a\Delta T + b\,, \tag{1}$$

where, a and b are the regression coefficient and the ΔS intercept in the regression line, respectively.

The simplified expression for the static stability of E is written as follows[10]:

$$E \approx \left(\frac{\partial \sigma_T}{\partial T}\frac{dT}{dZ} + \frac{\partial \sigma_T}{\partial S}\frac{dS}{dZ}\right) \times 10^{-3}\,, \tag{2}$$

where, $E=(\partial\sigma_T/\partial Z)\times 10^{-3}$ g cm^{-4} and σ_T is the density in sigma-t. Using $\alpha=(\partial\sigma_T/\partial T)\times 10^{-3}$ g cm^{-3} °C^{-1} and $\beta=(\partial\sigma_T/\partial S)\times 10^{-3}$ g cm^{-3} ‰$^{-1}$, equation (2) is rewritten as follows:

$$E \approx \alpha\frac{dT}{dZ} + \beta\frac{dS}{dZ}\,. \tag{3}$$

In the equation above, values of α and β are parameters of the contribution to the density by heat and salt, respectively. Applying equation (3) to the inversion layer with a thickness of ΔZ, the following equation can be deduced.

$$\Delta S = \left(-\frac{\alpha}{\beta}\right)\Delta T + \frac{E\Delta Z}{\beta}\,. \tag{4}$$

The equation (4), showing the stability relationship, takes account of the contribution to the density by changes of temperature and salinity, and the last term implies the vertical stability of the inversion layer. A comparison of equations (1) and (4) shows that the coefficient a and the constant term b correspond to $(-\alpha/\beta)$ and $E\Delta Z/\beta$, respectively.

Table 2. *Values of static stability parameters. Values of a, b and r (correlation coefficient) are obtained from the regression rule of equation (1). Those of* $(-\alpha/\beta)$ *and* $E\Delta Z/\beta$ *are calculated from the stability relationship of equation (4).*

Date	Nos. of Layer	a	$(-\alpha/\beta)$	b	$(E\Delta Z/\beta)$	r
June						
1978, 9–10	17	0.18	0.11	0.15	0.22	0.79
1979, 21–22	23	0.24	0.12	0.08	0.22	0.89
Total	40	0.22	0.12	0.10	0.22	0.86
July						
1978, 19–20	18	0.25	0.16	0.15	0.24	0.81
1979, 23–24	21	0.19	0.17	0.21	0.24	0.63
Total	39	0.22	0.16	0.18	0.24	0.73
August						
1978, 25–26	20	0.24	0.17	0.05	0.11	0.81
1979, 16–17	5	0.17	0.20	0.12	0.10	0.90
Total	25	0.22	0.18	0.08	0.11	0.81

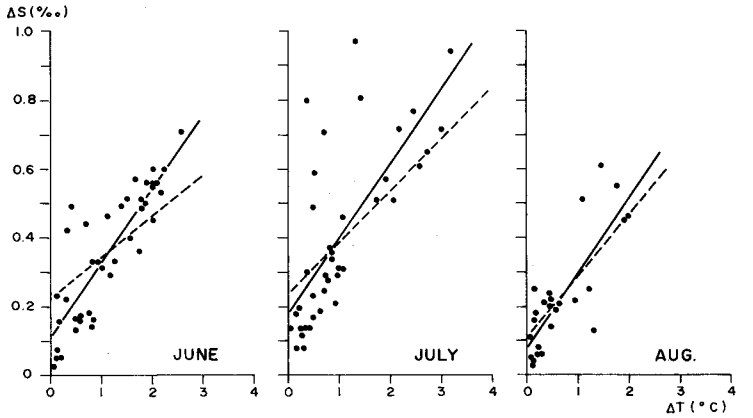

Fig. 9. Relationship between ΔT and ΔS of the temperature inversion layers for various periods. Solid and broken lines are calculated from the regression rule (1) and the stability relationship of equation (4), respectively.

These values are shown in Table 2. Values in September are omitted, since there was a lack of reliability due to few data, and no significant relationship could be found. The values of a varied from 0.17 to 0.25. However, comparing a with $(-\alpha/\beta)$, the former were about twice the latter in June, and these two values gradually got closer in July and August. The values of b were smaller by one-half in June and August than in July, and differed somewhat from the values of $E\Delta Z/\beta$ in June and July, but were similar in August. The correlation coefficient was the highest in June.

Fig. 9 shows these relationships. It can be seen that the slope and the ΔS intercept obtained using equation (1) were clearly different for those using equation

(4) in June and July, though the lines were closer in August. The large values of $E\Delta Z/\beta$ suggest that the large vertical gradient in salinity, which sufficiently compensated for the density decrease due to the increasing temperature, was present in June and July. The lack of agreement between equations (1) and (4) may be the result of this situation.

2. *Contribution of salinity to density stratification*

Taking ΔS_0 as the salinity difference which compensates for the density decrease due to the increasing temperature ΔT, and ΔS_1 as the remainder, *i.e.*, $\Delta S = \Delta S_0 + \Delta S_1$, equation (4) is transformed as follows:

$$E = \frac{1}{\Delta Z}(\alpha \Delta T + \beta \Delta S)$$

$$= \frac{1}{\Delta Z}\{\alpha \Delta T + \beta(\Delta S_0 + \Delta S_1)\}$$

$$= \frac{\beta}{\Delta Z}\Delta S_1 ,$$

where the relation $\alpha \Delta T + \beta \Delta S_0 = 0$ is assumed. Consequently, equation (4) finally becomes,

$$\Delta S = \left(-\frac{\alpha}{\beta}\right)\Delta T + \Delta S_1 . \tag{5}$$

Equation (5) replaces the last term of equation (4) with the salinity difference. This implies that the salinity difference consists of two parts; one compensates for the density decrease due to the increasing temperature and the other contributes to the density stratification in the inversion layer. Therefore, the remaining salinity difference, ΔS_1 must be identical to the last term in equation (4), $E\Delta Z/\beta$.

Now, let us assume ΔS_1 is proportional to ΔS, *i.e.*,

$$\Delta S_1 = k \Delta S \qquad (k < 1) .$$

Substituting it into (5), we obtain

$$\Delta S = \frac{\alpha}{\beta (k-1)}\Delta T \tag{6}$$

or

$$\beta \Delta S = \frac{1}{k-1}\alpha \Delta T . \tag{7}$$

Equation (7) shows the relationship between $\alpha \Delta T$ and $\beta \Delta S$ which takes account of the effect of salinity contribution on the density gradient, hence it is applicable to the temperature inversion generated under the condition of continuously increasing salinity. k indicates the ratio of the salinity difference

Table 3. *Values of k, ΔS_1 and k' for various periods.*

Date	Nos. of Layer	k	ΔS	ΔS_1	$E\Delta Z/\beta$	k'
June	40	0.58	0.36	0.21	0.22	0.61
July	39	0.51	0.41	0.21	0.24	0.56
August	25	0.37	0.22	0.08	0.11	0.50

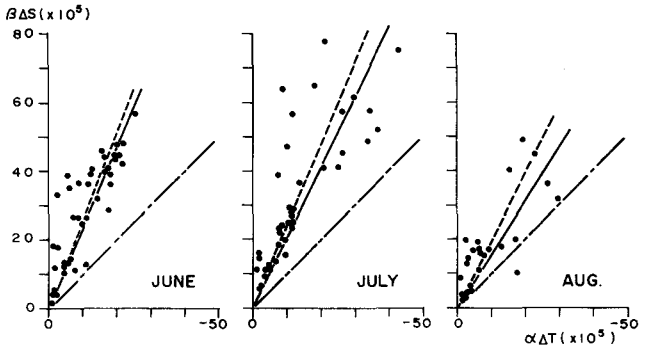

Fig. 10. Relationship between $\alpha\Delta T$ and $\beta\Delta S$ of the temperature inversion layers. Solid and broken lines are calculated from the regression rule and from equation (7) using k', respectively. Dot-dashed line indicates isopycnal inversion layer.

contributing to the density gradient to its total difference in the inversion layer. In the case of $k<0$ ($\Delta S<\Delta S_0$), the density decrease due to the increasing temperature has not yet been compensated for, and therefore a density inversion may arise in the temperature inversion layer. In the other case, $k=0$ ($\Delta S=\Delta S_0$), there is a neutral stability, in which case the inversion layer is isopycnal with the layer above.

The value of k is obtained from the slope of the regression line between $\alpha\Delta T$ and $\beta\Delta S$ that goes through the origin, using (7). The value of ΔS_1 can be estimated as the product of k and the observed ΔS, while, the similar value of k' is calculated by dividing $E\Delta Z/\beta$ by ΔS. These values are shown in Table 3. The value of k decreased gradually from 58% in June to 37% in August, and ΔS_1 in June and July were larger than in August. Hence, the slope of the regression line in August approached that of the dot-dashed isopycnal line as indicated in Fig. 10. ΔS_1 agreed with $E\Delta Z/\beta$ in all three months. The value of k' showed a tendency similar to that of k, as mentioned above.

Fig. 10 represents the relationship between $\alpha\Delta T$ and $\beta\Delta S$ in equiation (7) using the obtained k and k', and also the isopycnal line ($\alpha\Delta T=\beta\Delta S$). The lines which were deduced from the observed values of ΔS and $E\Delta Z/\beta$ agreed with the regression lines, and this suggests that the equation (7) may be relevant to a variety of oceanic conditions. In a similar way, Fig. 11 shows the regression lines between ΔT and ΔS, and the equation (6) using k'. The lines of Fig. 11 approached each other in all months, compared with those of Fig. 9.

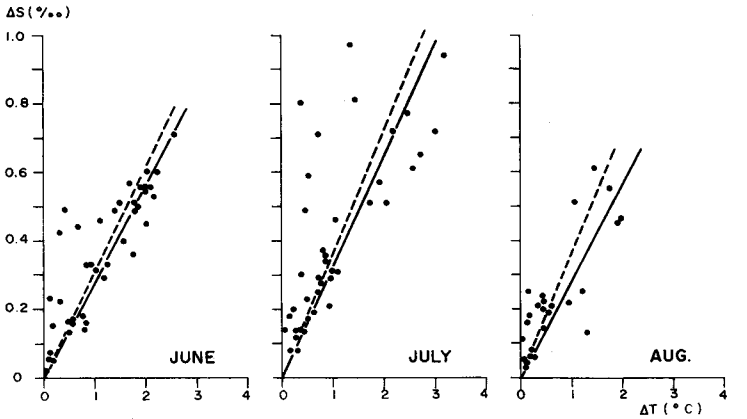

Fig. 11. Relationship between ΔT and ΔS of the temperature inversion layers. Solid and broken lines are calculated from the regression rule and from equation (6) using k', respectively.

Thus, the temperature inversion layers in June might be sufficiently compensated for by the large graident in salinity. This may be one of the reasons why the inversion layers that formed due to the inflow of O&Oi were stable enough to maintain conditions over a long term, from March to June. The fact that the large vertical gradient in density continued until July may provide a favourable condition for the development of horizontal intrusion as the inflowing pattern of Tw. Actually, the intrusive layer at 40 m to 60 m depth at Stns. 13 and 16 in Fig. 6 extended horizontally for more than 6 miles with a 10–20 m thickness.

Under constant vertical gradients in temperature and salinity, the intrusive layer caused by molecular diffusive processes is referred as double diffusive intrusion. In laboratory experiments, several analyses were made and some of them were compared with the field observations[11,12]. Even if the molecular processes occur on a small scale in the shallow water mentioned above, the vertical mixing may be intensified by this double diffusive convection and by the overturning convection due to surface cooling. Therefore, the deep mixing layer in autumn may be formed in a short time.

Acknowledgement

The author wishes to express his sincere thanks to Prof. J. Fukuoka, Associate Prof. M. Kajihara and Associate Prof. K. Ohtani for their criticisms and reading the manuscript of this work. Thanks are also due to Mr. H. Takeda, Mr. Y. Fujiyoshi, the former captain Mr. N. Sakaguchi and other crews of RV Ushio Maru for their kind cooperation on board.

References

1) Ohtani, K. and Y. Akiba (1970). Studies on the change of hydrographic conditions in the Funka Bay. I. The annual change of the water of the bay. *Bull. Fac. Fish. Hokkaido Univ.*, **20**, 303–312.

2) Ohtani, K. (1971). *Ditto*, II. Characteristics of the water occupying the Funka Bay. *Ibid.* **22**, 58–66.
3) Ohtani, K., Y. Akiba, K. Yoshida and T. Ohtsuki (1971). *Ditto*, III. Oceanographic conditions of the Funka Bay occupied by the Oyashio waters. *Ibid.* **22**, 129–142.
4) Ohtani, K., Y. Akiba, E. Ito and M. Onoda (1971). *Ditto*, IV. Oceanographic conditionds of the Funka Bay occupied by the Tsugaru Warm waters. *Ibid.* **22**, 221–230.
5) Ohtani, K. and K. Kido (1980). Oceanographic structure in Funka Bay. *Ibid.* **31**, 84–114.
6) Miyake, H. (1978). A simple temperature-gradient meter and its application to the small scale thermal structure in the coastal zone. *Ibid.* **29**, 270–281.
7) Ohtani, K. and R. Deguchi (1981). Coastal upwelling off the eastern coast of the Oshima Peninsula-I. *Ibid.* **32**, 77–96.
8) Fedorov, K.N. (1978). *The thermohaline finestructure of the ocean*, (English translation), 170p, Pergamon Press, Oxford.
9) Fedorov, K.N. (1969). On the vertical stability of temperature inversions in the ocean. *Okeanologiya*, **9**, 82–86.
10) Howe, M.R. and R.I. Tait (1972). The role of temperature inversions in the mixing processes of the deep ocean. *Deep-Sea Res.*, **19**, 781–791.
11) Turner, J.S. (1978). Double-diffusive intrusions into a density gradient. *J. Geophys. Res.*, **83**, 2887–2901.
12) Ruddick, B.R. and J.S. Turner (1979). The vertical length scale of double-diffusive intrusions. *Deep-Sea Res.*, **26**, 903–913.